

Effects of Boron Purity, Mg Stoichiometry and Carbon Substitution on Properties of Polycrystalline MgB_2

R. A. Ribeiro, S. L. Bud'ko, C. Petrovic, P. C. Canfield

*Ames Laboratory and Department of Physics and Astronomy
Iowa State University, Ames, IA 50011 USA*

Abstract

By synthesizing MgB_2 using boron of different nominal purity we found values of the residual resistivity ratio ($RRR = R(300K)/R(42K)$) from 4 to 20, which covers almost all values found in literature. To obtain high values of RRR , high purity reagents are necessary. With the isotopically pure boron we obtained the highest $RRR \sim 20$ for the stoichiometric compound. We also investigated $\text{Mg}_x^{11}\text{B}_2$ samples with $0.8 < x < 1.2$. For the range $\text{Mg}_{0.8}^{11}\text{B}_2$ up to $\text{Mg}_{1.2}^{11}\text{B}_2$ we found average values of RRR between 14 and 24. For smaller variations in stoichiometry ($x = 1 \pm 0.1$) $RRR = 18 \pm 3$. All of our data point to the conclusion that high RRR (~ 20) and low ρ_0 ($\leq 0.4 \mu\Omega\text{cm}$) are intrinsic material properties associated with high purity MgB_2 . In addition we have performed initial work on optimizing the formation of carbon doped MgB_2 via the use of B_4C . Nearly single phase material can be formed by reaction of nominal $\text{Mg}(\text{B}_{0.8}\text{C}_{0.2})_2$ for 24 hours at 1200°C . The T_c for this composition is between 21.9K and 22.7K (depending on criterion).

Key words: MgB_2 , stoichiometry, transport properties

PACS: 74.70.Ad, 74.25.Fy

1 Introduction

Since the discovery of superconductivity in the compound MgB_2 by Akimitsu and co-workers [1,2], considerable progress has been made in the understanding of the fundamental properties of this material. Within weeks of the announcement of this discovery, it was established that high purity, very low residual resistivity samples of MgB_2 could be synthesized by exposing boron powder or filaments to Mg vapor at temperatures at or near 950°C for as little as two hours [3,4,5]. Samples with residual resistivity ratio [$RRR = R(300K)/R(42K)$] values in excess of 20 and residual resistivities as

low as $0.4 \mu\Omega cm$ were synthesized by this method. Such a low resistivity in an intermetallic compound with a superconducting critical temperature, T_c , near $40K$ was of profound physical, as well as engineering, interest. The implications of this high RRR and low ρ_0 ranged from large magneto-resistances to questions of how a material with such an apparently large electron-phonon coupling could have such a small normal state resistivity. On the applied side, a normal state resistivity of $0.4 \mu\Omega cm$ for temperatures just above T_c means that MgB_2 wires would be able to handle a quench with much greater ease than, for example, Nb_3Sn wires which have a ρ_0 that is over an order of magnitude larger for $T \sim 20K$ [5]. Unfortunately, other techniques of synthesizing MgB_2 had difficulties in achieving such high RRR or low ρ_0 values [6,7,8,9,10]. In some cases, the authors of these papers have concluded that the resistivity of their samples must be the intrinsic resistivity and that higher RRR values or lower residual resistivity values must somehow be extrinsic. In order to address these concerns and in order to shed some light on how low resistivity samples can be grown, we have studied the effects of boron purity and magnesium stoichiometry on sintered pellet samples. Based on these measurements, we conclude that the purity of the boron used to make the MgB_2 is a dominant factor in determining the ultimate, low temperature, normal state resistivity of the sample, and that RRR values as high as 20 and residual resistivities as low as $0.4 \mu\Omega cm$ are intrinsic materials properties of high purity MgB_2 [11].

Once reproducible synthesis of high purity, single phase, MgB_2 is understood and believed to be somewhat controllable, the next question to be addressed is: can MgB_2 be doped in a reliable manner? Whereas the effects of Al substitution for Mg were addressed very early on [12,13,14], substitutions on the boron site have been somewhat more difficult. There have been some attempts to substitute carbon for boron [15,16,17,18] with results varying from very little effect on T_c [15] to shift of T_c down to $\sim 35K$ [16,17] or $32K$ [18] depending upon the nominal carbon concentration as well as the sample synthesis route. By far the most appealing route to producing carbon doped MgB_2 is to start with the carbon mixed with the boron on the length scale of a unit cell. Starting with a boron rich compound such as B_4C appears to offer just such a route [18]. In order to determine how to synthesize as close to a single phase sample as possible we have measured powder X-ray diffraction spectra as well as temperature dependent magnetic susceptibility and electrical transport on a series of samples synthesized at different temperatures.

2 Sample synthesis

Samples of MgB_2 for this study were made in the form of sintered pellets. The sintered pellets were made by sealing stoichiometric amounts of $Mg(99.9\%)$ and B into Ta tubes, placing these tubes (sealed in quartz) into furnaces

heated to 950°C for 3 hours, and then quenched to room temperature [3]. For the initial studies of the effects of boron purity, stoichiometric MgB_2 was synthesized and the quality of the boron was varied. For the studies of magnesium stoichiometry, nominal stoichiometries that ranged from $\text{Mg}_{0.8}^{11}\text{B}_2$ to $\text{Mg}_{1.2}^{11}\text{B}_2$ were used and samples were synthesized with 99.95% pure, isotopically enriched ^{11}B [11].

Given that our synthesis technique involves a reaction between solid boron and Mg vapor we felt that any attempt at boron site substitution required that the dopant and the boron be mixed at an atomic level before exposure to Mg vapor. The compound B_4C is ideal given that it is boron rich and includes carbon - a likely dopant. Earlier work [18] indicated this may be a viable route, but also appeared to be somewhat preliminary. The carbon doped MgB_2 sintered pellets were made by sealing lumps of Mg (99.9%) and B_4C (99% - Alfa Aesar) into Ta tubes, following same procedure for the pure MgB_2 , and heating to a variety of temperatures. For this work, the samples were heated for 24 hours to four different temperatures: (750°C , 950°C , 1100°C , 1200°C). In order to compare our samples with the initial studies using B_4C as starting reagent (Mickelson *et al.* [18]), we also prepared samples by heating to 600°C for 2 hours and then 700°C for 2 more hours. The initial stoichiometric ratio in all these procedures was 5:2 of Mg: B_4C giving a nominal composition of $\text{Mg}(\text{B}_{0.8}\text{C}_{0.2})_2$.

A.C. electrical resistance measurements were made using Quantum Design MPMS and PPMS units. Platinum wires for standard four-probe configuration were connected to the samples with Epotek H20E silver epoxy. LR 400 and LR 700 A.C. resistance bridges were used to measure the resistance when the MPMS units were used to provide the temperature environment. Powder X-ray diffraction measurements were made using a $\text{Cu } K_{\alpha}$ radiation in a Scintag diffractometer and a Si standard was used for all runs. The Si lines have been removed from the X-ray diffraction data, leading to apparent gaps in the powder X-ray spectra.

3 Effects of Boron Purity

Figure 1 presents powder X-ray diffraction spectra for three samples with varying nominal boron purities: 90% purity, 99.99% purity, and the 99.95% purity, isotopically pure ^{11}B . By comparing the two upper panels to the bottom panel it can be seen that the strongest MgB_2 lines are present in all three samples. The spectrum shown in the upper panel, the data taken on the sample made from boron with only a 90% nominal purity, also has weak Mg and MgO lines present. This is not inconsistent with the fact that the primary impurity in the 90% boron is associated with Mg.

Figure 2 displays the normalized resistance, $R(T)/R(300K)$, of MgB_2 pellets that were made using the five different types of boron powder as described in Table 1. Each curve is the average of three resistance curves taken on different pieces broken off of each pellet. Figure 2 demonstrates that RRR values can range from as low as 4 to as high as 20 depending upon what source of boron is used. Among the natural boron samples examined there is a steady increase in RRR as the purity of the source boron is improved. The MgB_2 synthesized from the isotopically pure boron appears to have the best RRR , although its nominal purity is somewhat less than that of the 99.99% pure natural boron, but those skilled in the art will realize that claims of purity from different companies can vary dramatically. In addition, it is likely that the isotopically pure boron was prepared in a somewhat different manner from the other boron powders used (very likely using a boron fluoride or boric acid or any of its complexes as an intermediate phase, in order to achieve isotopic separation). The primary point that figure 2 establishes is that the purity of the boron used can make a profound difference on the normal state transport properties.

In Fig. 3 the same resistance data is plotted, but instead of simply normalizing the data at room temperature the data is normalized to the temperature derivative at room temperature. This is done to see if the resistance curves differ only by a temperature independent residual resistivity term: i.e. this normalization is based upon the assumption that the slope of the temperature dependent resistivity at room temperature should be dominated by phonon scattering, and therefore be the same for each of these samples. As can be seen, this seems to be the case, at least to the first order. By using higher purity boron we are able to diminish the additive, residual resistance by a factor of approximately five.

The insets to figs. 2 and 3 indicate that there is a monotonic improvement in T_c as the boron purity (or RRR value) is increased. T_c values vary from just below $38K$ to just above $39K$ depending upon which boron is used. It should be noted that similar behavior have been seen in other polycrystalline samples with poor RRR values [6,7,8,9,10].

Based upon these results, we choose the isotopically pure ^{11}B for the further study of the effects of Mg stoichiometry on MgB_2 pellet samples. But before we proceed to the next section, it is worth noting that one of the difficulties associated with the samples made by other research groups may well be due to the use of boron with less than the highest purity. In addition, to our knowledge very few other groups have been using the Eagle-Picher isotopically pure boron in the samples for electrical transport measurements. It should be noted though that recent measurements[19] have reproduced these results using Eagle-Picher ^{11}B .

4 Effects of Magnesium Stoichiometry

In order to study the effect of magnesium stoichiometry on the transport properties of Mg^{11}B_2 , a series of $\text{Mg}_x^{11}\text{B}_2$ ($0.8 \leq x \leq 1.2$) samples were synthesized. Figure 4 presents powder X-ray diffraction patterns for the extreme members of the series (top and bottom panels) as well as for the stoichiometric Mg^{11}B_2 (middle panel). In all cases the lines associated with the Mg^{11}B_2 phase are present. For the $\text{Mg}_{0.8}^{11}\text{B}_2$ sample, there is a weak line seen at $2\theta = 35.8^\circ$ that is associated with MgB_4 (marked with a +). This is consistent with the fact that there was insufficient Mg present to form single phase Mg^{11}B_2 . For the $\text{Mg}_{1.2}^{11}\text{B}_2$ sample there are strong diffraction lines associated with Mg (marked with *). This too is consistent with the stoichiometry of the sample: Mg^{11}B_2 is the most Mg-rich member of the binary phase diagram, therefore any excess Mg will end up as unreacted Mg. The X-ray diffraction pattern for the stoichiometric Mg^{11}B_2 shows much smaller peaks associated with a small amount of both MgB_4 and Mg phases. This pattern is different from the one shown in Fig. 2 in that this sample was reacted for 3 hours, whereas the sample used in Fig. 1 was reacted for 4 hours. Given that all of the samples used for the Mg-stoichiometry study were reacted for 3 hours, it is appropriate to show this powder diffraction set along with the other members of the series. It should be noted that there is continuous change in the nature of the second phases in the samples. For Mg deficient samples there is only MgB_4 as a second phase. For the stoichiometric Mg^{11}B_2 samples there are either no second phases or very small amounts of both MgB_4 and Mg (depending upon reaction times), and for the excess Mg samples there is no MgB_4 , but clear evidence of excess Mg.

Figure 5 presents normalized resistance data for five representative $\text{Mg}_x^{11}\text{B}_2$ pellets. In each case the curve plotted is the average of three or more samples cut from the same pellet. There is far less variation between the different pellets in this case than there was for the case of boron purity (Fig. 2). This is most clearly illustrated by the fact that the values of the $R(T)$ collapse almost completely onto a single manifold as viewed on full scale. Figure 6 plots the RRR values for each of the individual samples (shown as the smaller symbols) as well as the RRR of the average curve. As can be seen, the RRR values increase slowly from ~ 14 for $\text{Mg}_{0.8}^{11}\text{B}_2$ to ~ 18 for Mg^{11}B_2 . This is followed by an increase in RRR values for excess Mg, with $\text{Mg}_{1.2}^{11}\text{B}_2$ having an RRR value of ~ 24 . The important point to note is that even, for the most Mg deficient sample, the lowest measured RRR value is significantly greater than 10. At no point in this series we find samples with RRR values of 3, 6, or 10, even when a clear MgB_4 second phase is present. For samples ranging from $\text{Mg}_{0.9}^{11}\text{B}_2$ to $\text{Mg}_{1.1}^{11}\text{B}_2$ (dotted box in figure 6) the average RRR values cluster around $RRR = 18 \pm 3$. These data indicate that, for sintered pellets, RRR values of 18 can be associated with stoichiometric Mg^{11}B_2 in pellet form.

Whereas the effects of excess Mg are relatively minor in these samples (given their low intrinsic resistivities), these effects can still be clearly seen. In addition to the increase in the RRR value, there is a change in the form of the temperature dependence of the resistance. This can be best seen in Fig. 7, in which the resistance data have been normalized to its room temperature slope. The data for all x values less than 1.0 are similar (to within small differences in residual resistivity) and can be collapsed onto a single curve. On the other hand, the resistance data for the $x = 1.1$ and $x = 1.2$ are qualitatively different. They start out with somewhat higher normalized resistance data than the stoichiometric sample, and then below $100K$ cross below the stoichiometric sample. This is shown in Fig. 7 by representing the data for $x = 1.2$ as a dashed line and can also be seen in the inset (stars). This change in behavior is very likely due to the increasing effects of having Mg in parallel (and series) with the MgB_2 grains. As can be seen in Fig. 7, this effect becomes larger as the amount of excess Mg is increased. This deviation from the MgB_2 resistance curve may actually serve as a diagnostic for the detection of excess Mg.

For further details about the effects of boron purity, Mg stoichiometry or the results of our studies on MgB_2 wires segments see reference [11].

5 Carbon doping

Figure 8 presents the powder X-ray diffraction patterns for nominal $Mg(B_{0.8}C_{0.2})_2$ samples reacted for 24 hours at temperature of 750, 950, 1100 and $1200^\circ C$. The top pattern is from a sample that was reacted for 2 hours at $600^\circ C$ and then reacted for 2 more hours at $700^\circ C$. This sample was made using the temperature / time schedule outlined in reference [18] and serves as a point of comparison. There is a clear decrease in the signal coming from impurity phases in the material as the reaction temperature is increased. The reactions carried out at either 1100 or $1200^\circ C$ appear to be approaching single phase.

The temperature dependent magnetic susceptibility and electrical resistance for these samples are presented in Figs. 9 and 10 respectively. As the phase purity of the material is improving the onset temperature (see insets) decreases and the transition sharpens. The sample synthesized at $1200^\circ C$ for 24 hours has $T_c = 22.7K$ based on zero resistance criterion and $T_c = 21.9K$ based on an onset of diamagnetism criterion. It should be noted that, based on the magnetization data, for the sample synthesized at $950^\circ C$ the majority of the sample appears to have a $T_c \sim 16K$, well below the onset temperature of $23.5K$. This, as well as the other transition temperatures found for samples reacted at $750^\circ C$ or lower temperature may well be associated with inhomogeneities in these samples and may indicate that even further carbon doping

levels are possible. In addition, there is still a slight increase in T_c when the reaction temperature is increased from $1100^\circ C$ to $1200^\circ C$. This may indicate that a further increase in reaction time or temperature will yield some further (slight) increase in T_c . These data represent a first step in the optimization and study of carbon doped MgB_2 with the nominal composition of $Mg(B_{0.8}C_{0.2})_2$. A more detailed study is part of an ongoing research project.

6 Conclusion

In summary, through the synthesis of various MgB_2 samples with different nominal boron purities we found values of RRR from 4 to 20, which covers almost all values found in literature. To obtain high values of RRR , high purity reagents are necessary. With the isotopically pure boron we obtained the highest $RRR \sim 20$ for the stoichiometric compound. We also investigated $Mg_x^{11}B_2$ samples with $0.8 < x < 1.2$. These have shown that from the most Mg deficient samples we observe inclusions of the MgB_4 phase, and no evidence of Mg. For samples with excess Mg we do not observe any MgB_4 . For the range $Mg_{0.8}^{11}B_2$ up to $Mg_{1.2}^{11}B_2$ we found average values of RRR between 14 and 24. For smaller variations in stoichiometry ($x = 1 \pm 0.1$) $RRR = 18 \pm 3$. All of our data point to the conclusion that high RRR (≥ 20) and low ρ_0 ($\leq 0.4 \mu\Omega cm$) are intrinsic materials properties associated with high purity MgB_2 [11].

Our initial work on optimizing the formation of carbon doped MgB_2 via the use of B_4C indicates that nearly single phase material can be formed by reaction of nominal $Mg(B_{0.8}C_{0.2})_2$ for 24 hours at $1200^\circ C$. The T_c for this composition is between $21.9K$ and $22.7K$ (depending on criterion for T_c used). Further work on the optimization and characterization of this compound is ongoing, but it appears that $Mg(B_{0.8}C_{0.2})_2$ may offer a very useful window on the rather novel physics associated with MgB_2 .

Acknowledgements

Ames Laboratory is operated for the US Department of Energy by Iowa State University under Contract No. W-7405-Eng-82. This work was supported by the Director for Energy Research, Office of Basic Energy Sciences. The authors would like to thank N. Kelson for drawing our attention to earlier research on the properties of MgB_2 [20], M. A. Avila, D. K. Finnemore and N.E. Anderson, Jr. for helpful assistance and many fruitful discussions.

References

- [1] J. Akimitsu, Symposium on Transition Metal Oxides, Sendai, January 10, 2001.
- [2] J. Nagamatsu, N. Nakagawa, T. Muranaka, Y. Zenitani and J. Akimitsu, *Nature* 410 (2001) 63.
- [3] S. L. Bud'ko, G. Lapertot, C. Petrovic, C. E. Cunningham, N. Anderson and P. C. Canfield, *Phys. Rev. Lett.* 86 (2001) 1877.
- [4] D. K. Finnemore, J. E. Ostenson, S. L. Bud'ko, G. Lapertot and P. C. Canfield, *Phys. Rev. Lett.* 86 (2001) 2420.
- [5] P. C. Canfield, D. K. Finnemore, S. L. Bud'ko, J. E. Ostenson, G. Lapertot, C. E. Cunningham and C. Petrovic, *Phys. Rev. Lett.* 86 (2001) 2423.
- [6] X. H. Chen, Y. S. Wang, Y. Y. Xue, R. L. Meng, Y. Q. Wang and C. W. Chu, *Phys. Rev. B* 65 (2002) 024502.
- [7] Sang Young Lee, J. L. Lee, Jung Hun Lee, J. S. Ryu, J. Lim, S. H. Moon, H. N. Lee, H. G. Kim and B. Oh, *Appl. Phys. Lett.* 79 (2001) 3299.
- [8] A. K. Pradhan, Z. X. Shi, M. Tokunaga, T. Tamegai, Y. Takano, K. Togano, H. Kito and H. Ihara, *Phys. Rev. B* 64 (2001) 212509.
- [9] Kijoon H. P. Kim, Jae-Hyuk Choi, C. U. Jung, P. Chowdhury, Hyun-Sook Lee, Min-Seok Park, Heon-Jung Kim, J. Y. Kim, Zhonglian Du, Eun-Mi Choi, Mun-Seog Kim, W. N. Kang, Sung-Ik Lee, Gun Yong Sung, Jeong Yong Lee, *Phys. Rev. B* 65 (2002) 100510.
- [10] Y. Y. Xue, R. L. Meng, B. Lorenz, J. K. Meen Y. Y. Sun and C. W. Chu, *Physica C* 377 (2002) 7.
- [11] R. A. Ribeiro, C. Petrovic, S. L. Bud'ko and P. C. Canfield, *Physica C* 382 (2002) 194.
- [12] J. S. Slusky, N. Rogado, K. A. Regan, M. A. Hayward, P. Khalifah, T. He, K. Inumaru, S. Loureiro, M. K. Hass, H. W. Zandbergen and R. J. Cava, *Nature* 410 (2001) 343.
- [13] B. Lorenz, R. L. Meng, Y. Y. Xue and W. Chu, *Phys. Rev. B* 64 (2001) 052513.
- [14] O. de la Peña, A. Aguayo and R. de Coss, *Phys. Rev. B* 66 (2002) 012511.
- [15] M. Paranthaman, J. R. Thompson and D. K. Chirsten, *Physica C* 355 (2001) 1.
- [16] J. S. Ahn and E. J. Choi, cond-mat/0103169.
- [17] T. Takenobu, T. Ito, D. H. Chi, K. Prassides and Y. Iwasa, *Phys. Rev. B* 64 (2001) 134513.
- [18] W. Mickelson, J. Cumings, W. Q. Han and A. Zettl, *Phys. Rev. B* 65 (2002) 052505.

- [19] V. Braccini, L. D. Cooley, S. Patnaik, P. Manfrinetti, A. Palenzona, A. S. Siri and D. C. Larbalestier, cond-mat/0208054.
- [20] L. I. Kostantinova, B. A. Katsnelson, L. K. Konysheva, N. N. Loboda, Current Toxicology 1 (1993) 23.

Table

Table 1: Boron form and purity (as provided by the seller).

Figures

Figure 1: Powder X-ray (Cu K_α radiation) diffraction spectra of stoichiometric MgB_2 (with h, k, l) for 3 different boron qualities (a) 90% pure natural boron; (b) 99.99% pure natural boron and (c) 99.95% pure isotopic enriched ^{11}B . Samples (a) and (b) were synthesized for $3h/950^\circ\text{C}$, and sample (c) for $4h/950^\circ\text{C}$. The data gaps are due to the removal of the Si peaks.

Figure 2: Variation of the normalized zero-field resistance as a function of temperature for MgB_2 pellets with different boron purities. Inset: expanded scale near T_c .

Figure 3: Resistance curves normalized by their temperature derivative at room temperature, for different boron purities. Inset: expanded scale near T_c .

Figure 4: X-ray spectra for 3 different nominal compositions of $\text{Mg}_x^{11}\text{B}_2$ for $x = 0.8, 1.0, 1.2$.

Figure 5: Temperature dependence of the normalized resistance for representative samples with nominal composition $\text{Mg}_x^{11}\text{B}_2$ ($0.8 < x < 1.2$). Inset: expanded scale near T_c .

Figure 6: Residual resistance ratio of $\text{Mg}_x^{11}\text{B}_2$ ($0.8 < x < 1.2$). The open symbols represent different pieces selected from the same batch. The solid symbols are the average. The dotted box delimits the smaller variation ($x = 1 \pm 0.1$).

Figure 7: Resistance curves normalized by temperature derivative at room temperature, for $\text{Mg}_x^{11}\text{B}_2$ ($x = 0.8, 0.9, 1.0, 1.1$ and 1.2). $x = 1.2$ data shown as dashed curve as discussed in the text. Inset: expanded scale near T_c .

Figure 8: Powder X-ray diffraction spectra of $\text{Mg}(\text{B}_{0.8}\text{C}_{0.2})_2$ (with h, k, l) for samples that were synthesized for (a) 2 hours at 600°C and then 2 hours at 700°C ; (b) 24 hours at 750°C ; (c) 24 hours at 950°C ; (d) 24 hours at 1100°C and (e) 24 hours at 1200°C . The data gaps are due to the removal of the Si peaks. Symbols: $+$ = B_4C , $*$ = MgB_2C_2 and $\#$ = Mg_2C_3 , as indicated in figure.

Figure 9: Temperature dependent magnetic susceptibility for representative $\text{Mg}(\text{B}_{0.8}\text{C}_{0.2})_2$ samples taken in $H = 50\text{Oe}$ applied field: ZFC - warming. Inset: expanded temperature range near T_c .

Figure 10: Normalized resistance as a function of temperature for $\text{Mg}(\text{B}_{0.8}\text{C}_{0.2})_2$ samples synthesized at different reaction temperatures. Inset: expanded temperature range near T_c .

Table 1

Purity	Form	Source	Main Impurities
90%	Amorphous (325 mesh)	Alfa Aesar	Mg 5%
95%	Amorphous (< 5 mesh)	Alfa Aesar	Mg 1%
98%	Crystalline (325 mesh)	Alfa Aesar	C 0.55%
99.95%	Isotopically pure ^{11}B Crystalline (325 mesh)	Eagle-Picher	Si 0.04%
99.99%	Amorphous (325 mesh)	Alfa Aesar	Metallic Impurities 0.005%

Figure 1

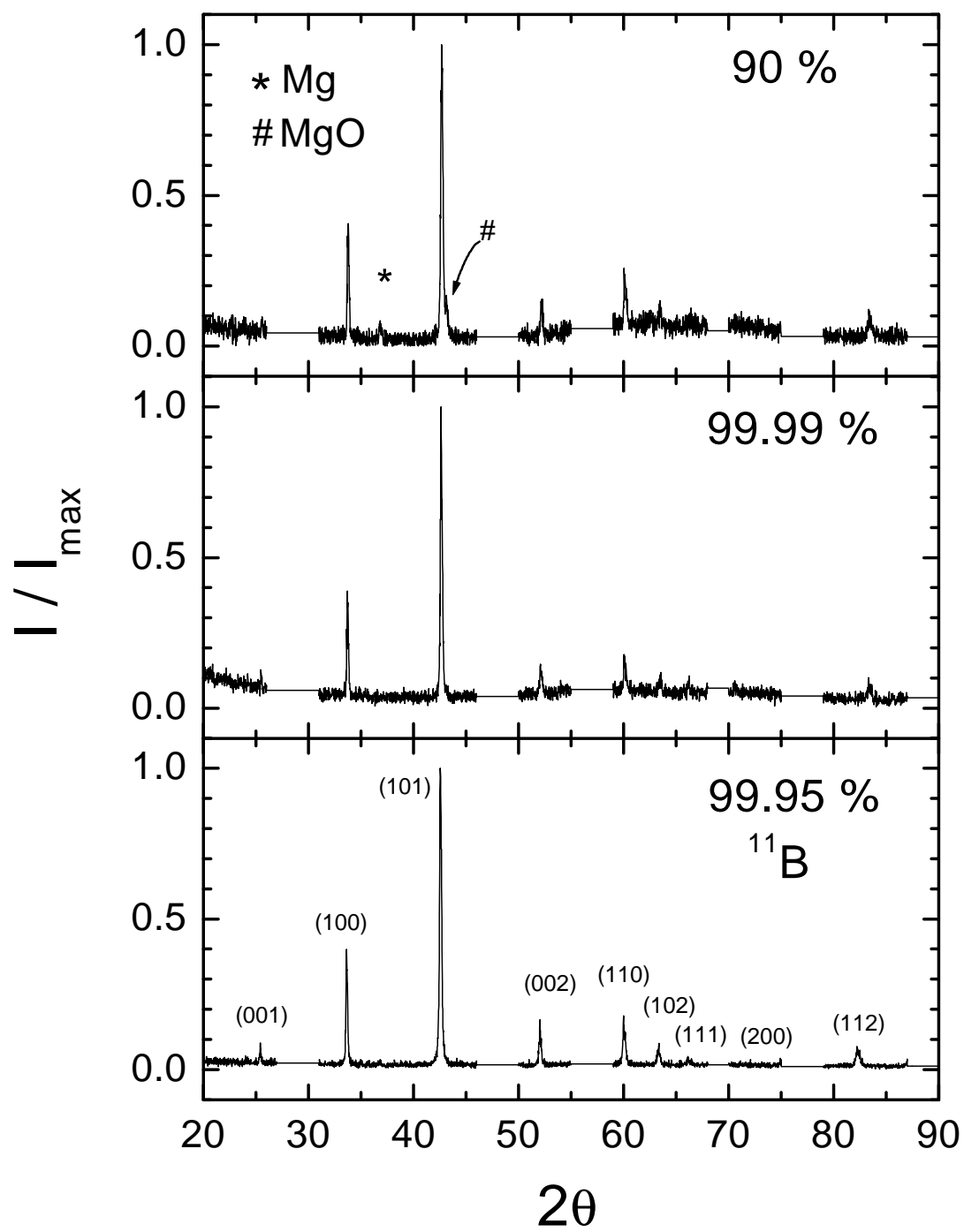


Figure 2

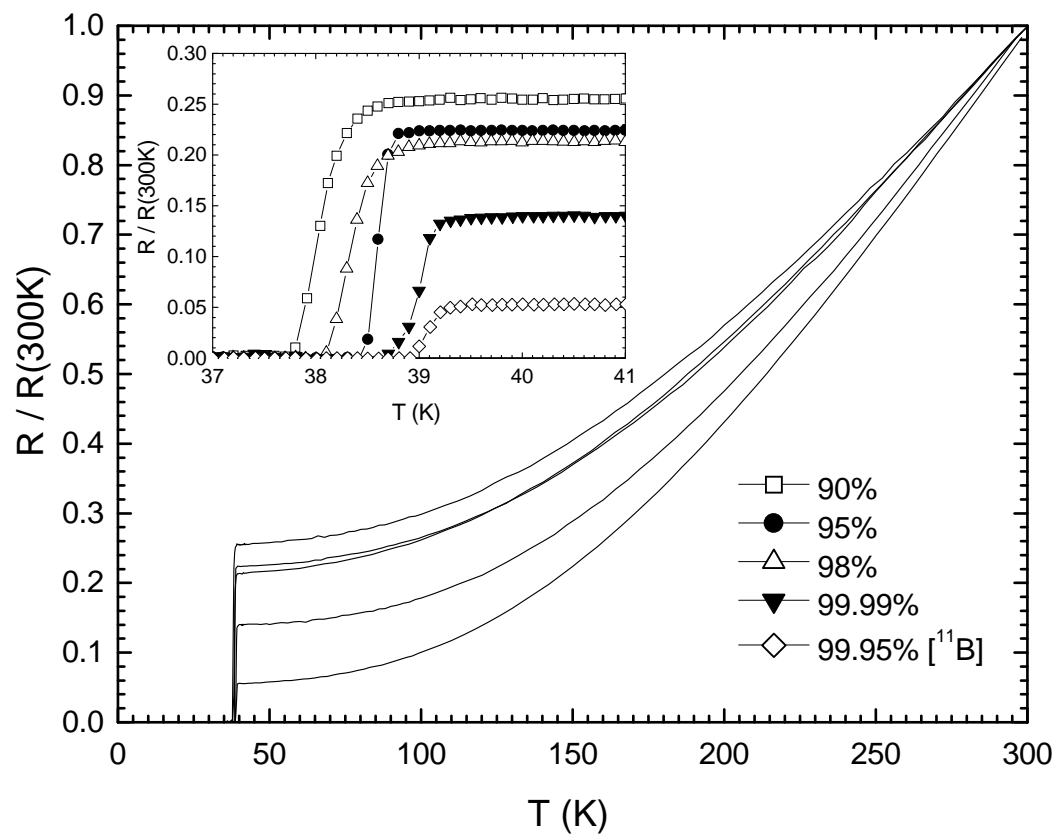


Figure 3

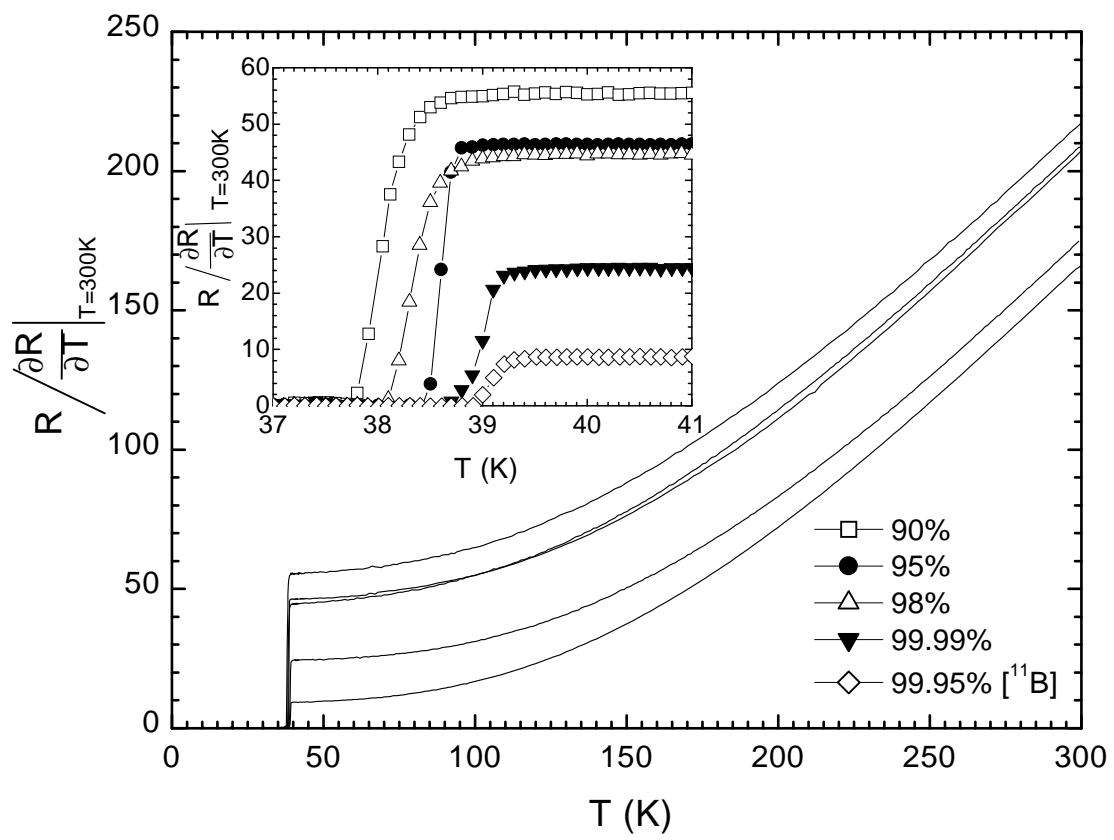


Figure 4

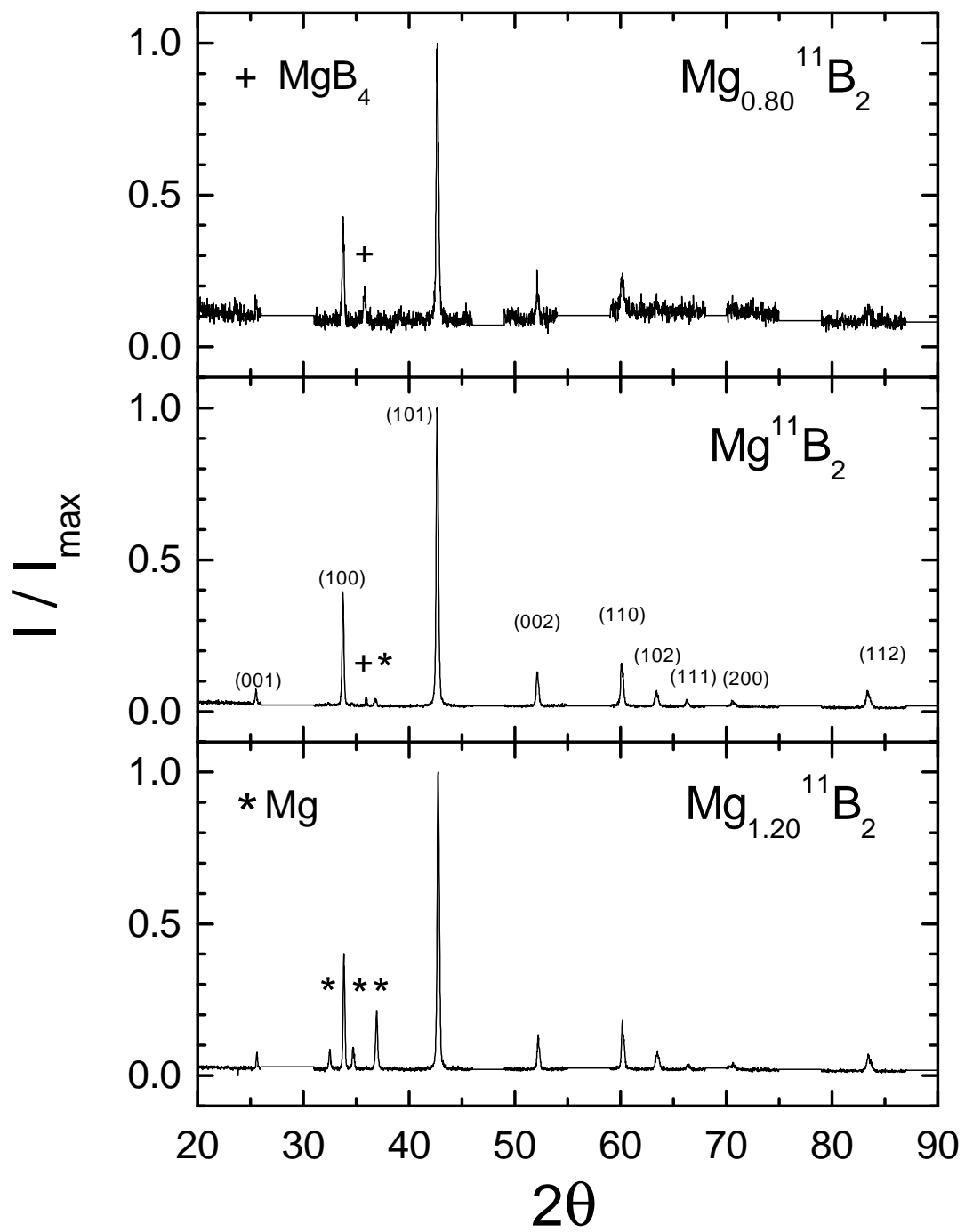


Figure 5

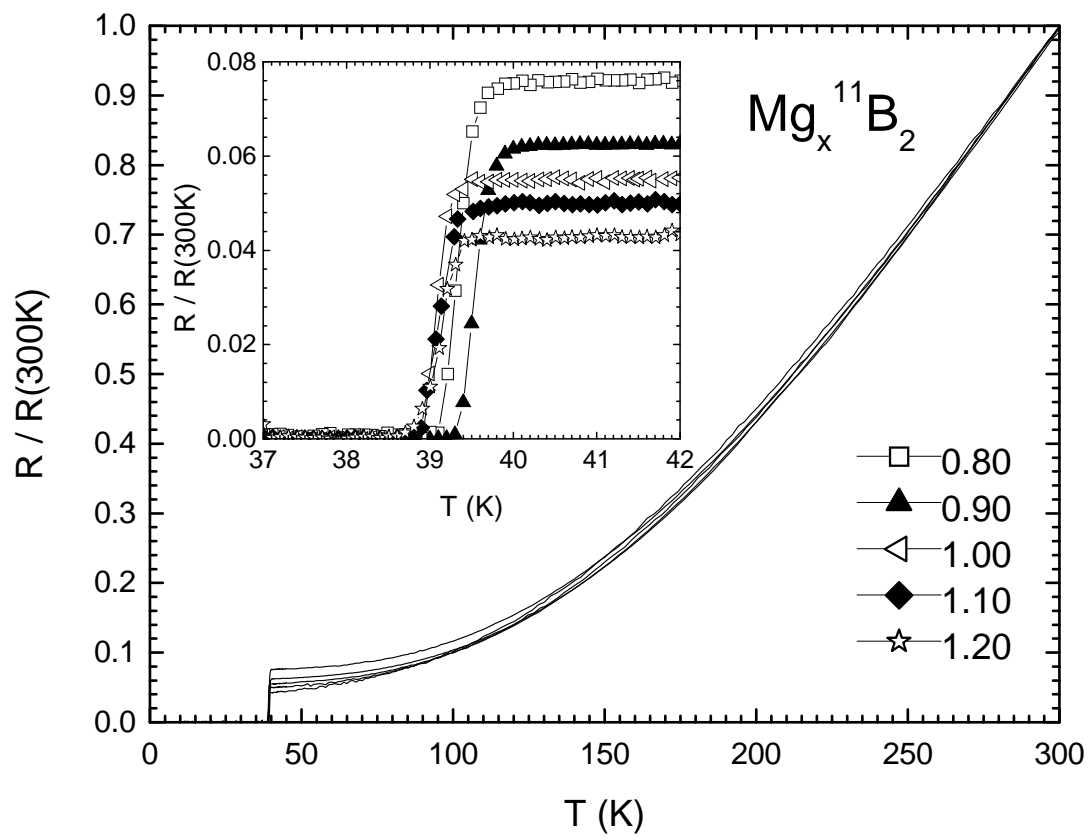


Figure 6

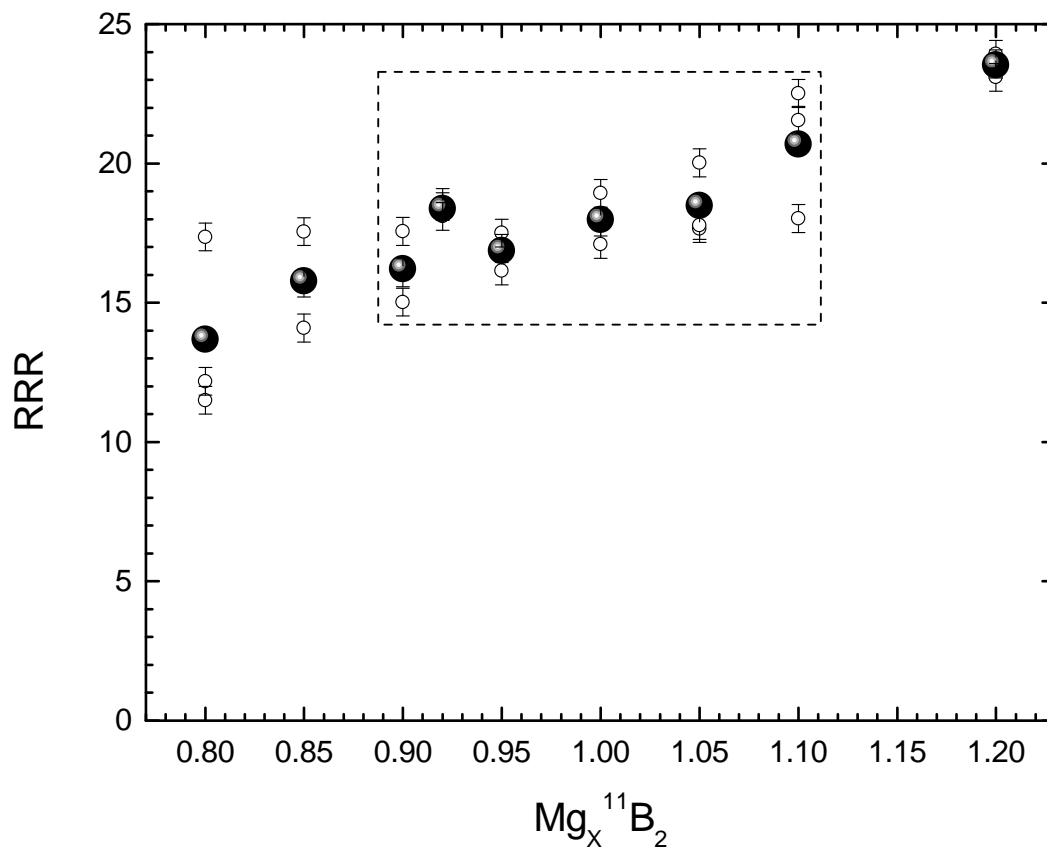


Figure 7

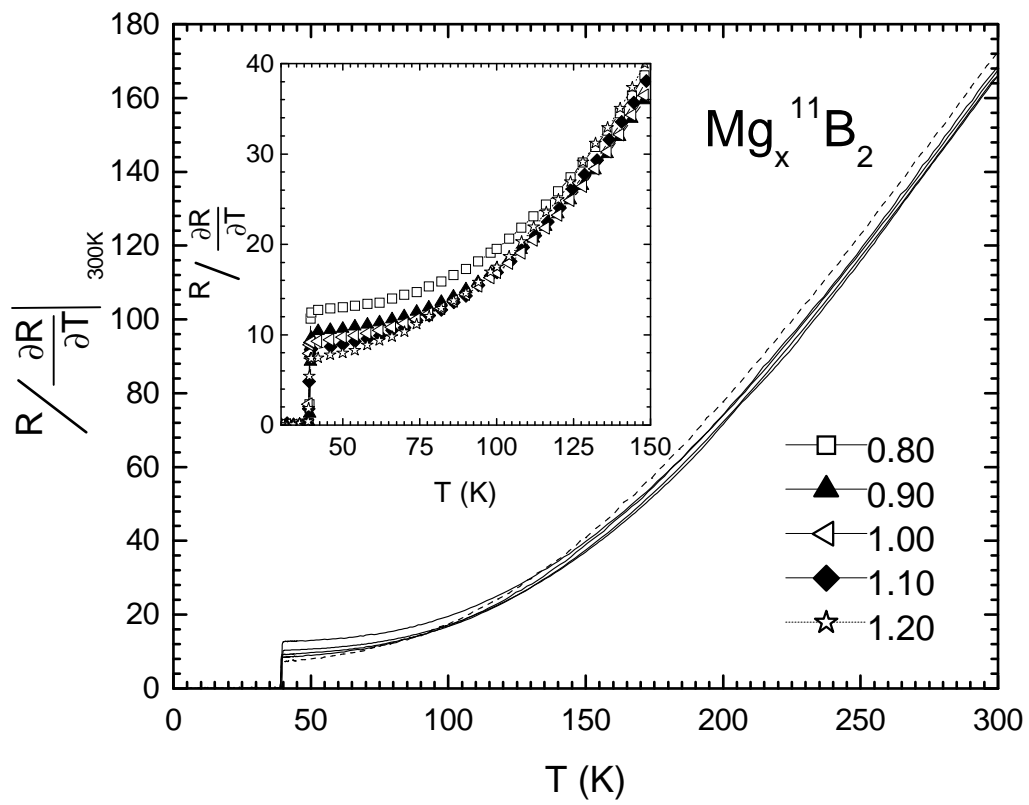


Figure 8

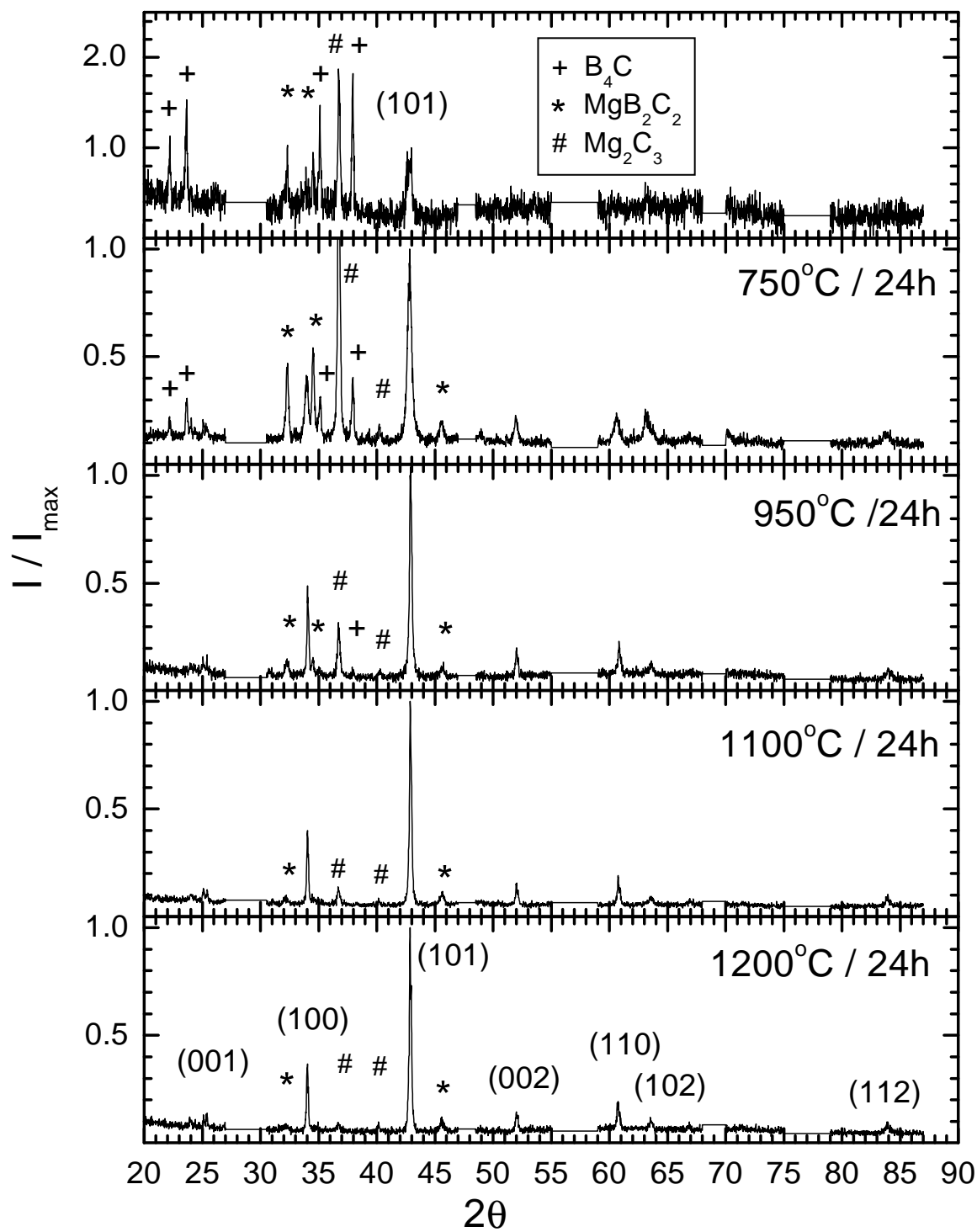


Figure 9

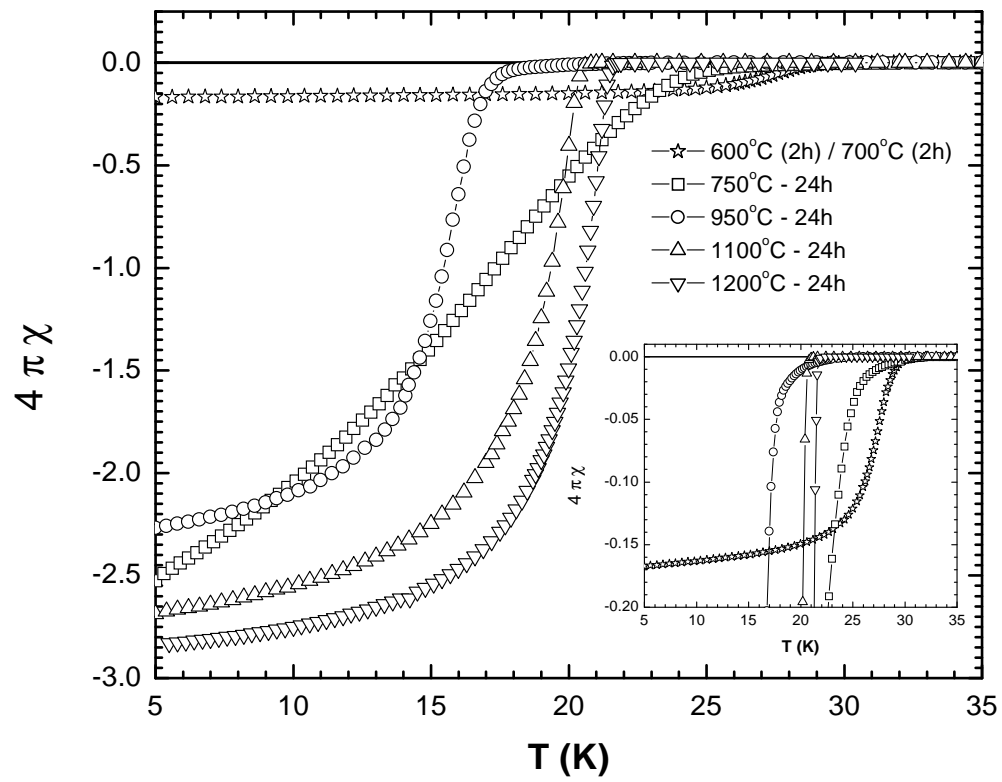


Figure 10

